Radiation Physics and Chemistry 242 (2026) 113647

Contents lists available at ScienceDirect

Radiation Physics and Chemistry

journal homepage: www.elsevier.com/locate/radphyschem

Feasibility assessment of an MR-based quantitative method for soft tissue elemental composition toward accurate BNCT dose calculation

Guolong Liu [a], Diyun Shu [b,*], Changran Geng [a,c,**], Xiaobin Tang [a,c], Yuan-Hao Liu [b,a], Yingzhi Zheng [d], Junhang Gao [d], Sulian Su [d], Youqun Lai [d]

[a] Department of Nuclear Science and Technology, Nanjing University of Aeronautics and Astronautics, Nanjing, PR China
[b] Neuboron Therapy System Ltd., Xiamen, Fujian Province, PR China
[c] Key Laboratory of Advanced Nuclear Technology and Radiation Protection, Ministry of Industry and Information Technology, Nanjing, PR China
[d] Xiamen Humanity Hospital, Xiamen, Fujian Province, PR China

ARTICLE INFO

Keywords:
Elemental composition
Mass fraction
MRI
BNCT
Soft tissue

ABSTRACT

The precise dose calculation in Boron neutron capture therapy (BNCT) heavily relies on accurate characterization of tissue elemental composition. However, current computed tomography (CT)-based methods face significant limitations in analyzing soft tissue elements due to the non-unique relationship between Hounsfield units (HU) and tissue parameters. A novel magnetic resonance imaging (MRI)-based quantitative analysis method to address this issue has been developed for deriving key elemental mass fractions (C, H, O, N) through measuring molecular components including water, lipids, and proteins. Using mDIXON-Quant MRI technology, the accuracy of fat quantification was first validated through phantom experiments (mean relative deviation <0.1 %) and established a linear calibration model between MRI signal intensity and water mass fraction. Further biological sample experiments demonstrated that MRI-derived mass fractions of H, N, and O agreed well with elemental analyzer measurements, whereas C quantification showed some data dispersion. Compared with traditional CT methods, MRI improved the prediction accuracy for C, H, and N elements. This study demonstrates the feasibility of MRI-based quantitative analysis, which may provide more accurate soft tissue elemental data for Monte Carlo simulations in BNCT treatment planning.

1. Introduction

Boron neutron capture therapy (BNCT) is an emerging targeted radiotherapy modality. The core mechanism relies on selectively delivering boron-10 (^{10}B) isotopes to tumor tissue, followed by irradiation with thermal or epithermal neutrons to trigger the ^{10}B(n,α)^{7}Li nuclear capture reaction. This reaction produces high linear energy transfer (LET) α particles and recoiling lithium nuclei (^{7}Li), which travel only 4–10 μm in biological tissue—approximately the diameter of a single cell. Owing to this highly localized energy deposition, BNCT achieves precise tumor cell destruction while sparing surrounding healthy tissues (Sauerwein et al., 2012; Barth et al., 1992, 2012, 2018).

In BNCT, the physical absorbed dose primarily consists of three components: the boron, neutron, and photon dose. The latter two results from nuclear interactions between neutrons and elements in human tissues (Kumada and Takada, 2018). Differences in tissue composition significantly influence neutron moderation, altering the spatial distribution of the neutron energy spectrum and thereby playing an important role in regulating the boron dose. Cross-sectional analysis based on the ENDF/B-VIII database shows notable variations in neutron reaction cross-sections among different nuclides, making tissue elemental composition a critical parameter in BNCT dose calculations. Studies indicate that tissue composition differences can lead to fluctuations exceeding 10 % in the maximum dose rate of normal tissues when evaluating the biological equivalent dose, while deviations in the physical absorbed dose assessment can reach up to 6 % (Teng et al., 2023). Therefore, the precise determination of tissue composition is essential to ensure reliable dose evaluation.

The Monte Carlo (MC) method (Andreo, 1991, 2018) is the standard approach for BNCT dose calculations and is widely used in treatment planning systems (TPSs). Currently, most TPSs rely on general-purpose MC codes (such as Geant4 (Grevillot et al., 2010)) to compute dose

* Corresponding author.
** Corresponding author. Department of Nuclear Science and Technology, Nanjing University of Aeronautics and Astronautics, Nanjing, PR China.
E-mail addresses: shudiyun@neuboron.com (D. Shu), gengchr@nuaa.edu.cn (C. Geng).

https://doi.org/10.1016/j.radphyschem.2026.113647
Received 30 July 2025; Received in revised form 23 December 2025; Accepted 14 January 2026
Available online 16 January 2026

distributions (Zhong et al., 2023), with the important input parameters being the elemental composition and mass density of each voxel derived from patient imaging data. In early studies, the human tissue elemental composition was primarily based on reference human models published by the International Commission on Radiation Units and Measurements/International Commission on Radiological Protection, using a homogeneous tissue assumption. However, this approach ignores tissue heterogeneity and inter-individual variations, which may introduce significant errors in dose calculations. To improve tissue characterization accuracy, Schneider et al. proposed a stoichiometric calibration method for computed tomography (CT)-number-to-Hounsfield-unit (HU) conversion (Schneider et al., 1996, 2000). However, this method has inherent limitations. Because HU values and tissue parameters do not have a strict one-to-one relationship, especially in soft-tissue regions, the low contrast in CT numbers reduces the reliability of calibration (Sudhyadhom, 2020). This highlights the need to develop more precise tissue characterization methods to improve the accuracy of BNCT dose calculations further. To improve the accuracy of elemental composition analysis, Teng et al. (2023) proposed a tissue parameter mapping method based on HU values. They divided the HU values into 96 discrete intervals to achieve a more precise matching. However, existing CT methods face a fundamental limitation in reconstructing elemental composition: the Hounsfield Unit (HU) lacks a stable, one-to-one correspondence with soft tissue elemental parameters. This intrinsic physical shortcoming, combined with the inherently low soft-tissue contrast in HU, makes it difficult to establish a reliable and generalizable signal-to-element quantitative model through stoichiometric calibration. Consequently, derivation errors are introduced, ultimately compromising the accuracy of BNCT dose calculations.

Given the limitations of conventional CT imaging in analyzing elemental composition in soft tissues, Saito et al. proposed a quantitative magnetic resonance imaging (MRI)-based method for measuring carbon (C) and oxygen (O) concentrations in soft tissues with the aim of improving the range verification accuracy in proton therapy. This method demonstrates lower prediction errors than conventional CT and provides better differentiation of brain tissues (Saito, 2023; Saito and Matsumoto, 2023). However, in BNCT, hydrogen (H) and nitrogen (N) are critical elements that affect dose calculations. Therefore, the potential of MRI in BNCT treatment planning was explored, and a "soft--tissue–molecular content–elemental mass fraction" framework was developed. This framework leverages MRI to quantify the mass fractions of water, lipids, and proteins directly or indirectly in soft tissues and then derives the elemental composition to establish a tissue parameter model for optimizing voxel parameter settings in MC simulations. This study provides a reference for expanding MRI applications in BNCT dose calculations and offers new methodologies to improve treatment planning accuracy.

2. Materials and methods

2.1. Theoretical framework: molecular-to-elemental mapping

Human soft tissues are primarily composed of water and organic molecules. O and H mainly exist as water molecules, whereas C serves as the backbone element of organic molecules and combines with H, O, N, and other atoms to form several biological macromolecules (Woodard and White, 1986). The following hypothesis is proposed: human soft tissues can be simplified as a system consisting of water and organic molecules. To validate this hypothesis, the dataset of 47 standard human soft tissues assembled by Hünemohr et al. (2014) was employed, and the mass fractions of water, lipids, and proteins were analyzed. Table 1 lists the mass fractions of these three components in selected soft tissues (their sum represents the total mass fraction). The results show that, except for cartilage and bile, water, lipids, and proteins account for more than 96 % of the mass fraction in most soft tissues. From a numerical analysis perspective, human soft tissues can be approximately considered as a ternary system composed of water, lipids, and proteins. This simplified model supports the first part of the proposed technical framework ("human soft tissues → molecular content").

Table 1
Reference tissue parameters of the standard human soft tissues (Schneider et al., 2000; Woodard and White, 1986).

Tissue	Water(w_{tw}) (mass%)	Lipid (mass%)	Protein (mass%)	Total mass fraction (mass%)
Kidney 1	72.3	6.9	19.9	99.1
Thyroid	78.4	4.4	14.0	96.8
Aorta	72.1	1.8	25.0	98.9
Heart 2	75.9	6.2	17.1	99.2
Kidney 2	76.6	4.8	17.7	99.1
Liver 1	72.8	7.8	16.1	96.7
Muscle, skeletal 2	74.1	4.2	19.8	98.1
Muscle, skeletal 3	78.6	1.6	17.9	98.1
Heart 3	80.9	2.4	15.9	99.2
Mammary, gland 3	72.6	5.6	21.5	99.7
Kidney 3	80.5	2.8	15.8	99.1
Ovary	82.8	2.3	14.0	99.1
Eye lens	64.1	2.0	33.6	99.7
Liver 2	74.5	4.6	17.6	96.7
Trachea	74.2	3.8	18.9	96.9
Spleen	78.7	1.8	18.6	99.1
Heart,blood-filled	77.7	2.8	18.6	99.1
Blood, whole	79.0	0.6	19.6	99.2

Since human soft tissues are simplified as a ternary system, and previous studies showed that the elemental composition and mass fractions of these three molecular components follow established biological patterns with relatively stable proportional distributions, the second part of the framework ("molecular content → elemental mass fractions"). Specifically, after the mass fractions of water, lipids, and proteins in soft tissues were measured quantitatively using MRI, the mass fractions of C, H, O, and N were calculated based on their stable elemental ratios. The elemental composition of human tissues was investigated systematically and the mass fractions of important elements (C, H, O, and N) in major components were quantified, including lipids, proteins, and water (Table 2). In the final calculation, proteins were represented using the standard average elemental composition. For lipid components, tissue-specific approaches were applied: brain tissue was modeled with a phospholipid composition, whereas other soft tissues used a triglyceride composition.

2.2. Magnetic resonance imaging sequences: technical introduction

Magnetic resonance (MR) technology primarily relies on H protons (^{1}H) in free water molecules and lipid molecules as signal sources. In this case, protons exhibit high mobility, with precession frequencies close to the MR central frequency of the MR system, making effective excitation and detection possible using radiofrequency (RF) pulses. In contrast, the H protons in protein molecules demonstrate restricted motion owing to molecular structural constraints, causing their frequencies to deviate significantly from the MR central frequency. Consequently, conventional MR imaging sequences cannot detect the proton signals. Based on these physical principles, the quantitative measurement of soft-tissue molecular composition was simplified to water and lipid mass fraction determination. By precisely measuring water and lipid mass fractions

Table 2
Elemental compositions of water, lipids, and proteins (Giera, 2020; Smith, 1966).

Components	Elemental composition (mass fraction)
Lipid (triglyceride)	H(11.8),C(77.4),O(10.8)
Lipid (phospholipid)	H(9.7),C(62.3),N(1.7),O(15.1),P(3.7)
Protein	H(6.6),C(53.4),N(17.0),O(22.0),S(1.0)
Water	H(11.2),O(88.8)

using MR technology, protein mass fractions can be derived indirectly.

Through systematic experimental validation and technical evaluation, the modified Dixon quantitative (mDIXON-Quant) method was identified as the core method for fat quantification. Data acquisition was performed using a Philips MRI system with the following sequence parameters: repetition time (TR)/echo time (TE) = 5.7/0.97 ms, number of excitations (NEX) = 1, field of view (FOV) = 450 mm, matrix size = 160 × 140, slice thickness = 2.5 mm, slice gap = 0 mm, number of slices = 12, and total scan duration = 36.5 s. This advanced MRI technique uses multi-echo acquisition and an optimized signal decomposition algorithm to generate high-resolution water and fat-only images simultaneously, making possible the precise calculation of the Proton Density Fat Fraction (PDFF) (Lins et al., 2021) (In the present work, PDFF was treated as equivalent to the fat mass fraction). Compared with the conventional Dixon method, this method significantly reduces quantification errors caused by magnetic field inhomogeneity, providing reliable measurements of tissue fat mass fraction. For water quantification, the water-only images from the mDIXON-Quant sequence is considered as the basis for analysis. By establishing a standardized calibration model that correlates the image signal intensity with known water concentrations, the MR signals were converted into actual water mass fraction values.

After the MRI sequence and technical protocol were finalized, the following experimental steps were used. 1. Fat phantom validation: A pre-made fat phantom system is used to verify the accuracy of fat quantification using the selected sequence. 2. Water phantom calibration: A standardized water phantom is used to establish a quantitative calibration model between image grayscale values and water concentration, while also evaluating water mass fraction measurement precision. 3. Biological sample analysis: The validated MRI platform used to quantify the elemental composition of biological soft-tissue samples. The results are compared with those of conventional CT measurements to assess the advantages of the proposed method.

2.3. Formulation of phantom solutions for technical validation

The fat phantom design employed in this study, based on the established protocols by Hernando et al. (2012, 2015, 2017), encompasses both water-only and agar-based oil–water emulsion phantoms to simulate the distinct distribution characteristics of water and lipids across biological tissues. The experimental setup consisted of nine cylindrical glass vials (25-mm diameter, 90-mm height). Each vial was filled with either aqueous solutions for water phantoms or stabilized oil-water emulsions for fat phantoms. The fat phantoms were formulated to cover a mass fraction gradient of 0 %, 5 %, 10 %, 15 %, 20 %, 30 %, 40 %, 50 %, and 100 %. This mass fraction range was selected in accordance with established validation protocols, as it comprehensively spans the physiological fat-content spectrum of human soft tissues—-from entirely fat-free to fully adipose regions. Hernando et al. (2012) demonstrated that a 0 %–100 % mass fraction gradient is essential for verifying the linearity and precision of advanced fat-quantification techniques such as mDIXON-Quant, and their subsequent multicenter study (2017) further validated this range as a reference standard for ensuring cross-platform consistency in MRI-based fat measurements. Each emulsion contained the following components (Fig. 1a): deionized water, peanut oil, agar (2 % w/v, as a gelling agent), sodium dodecyl sulfate (SDS, 43 mM, as an emulsifier), sodium chloride (43 mM, for ionic strength adjustment), sodium benzoate (3 mM, as a preservative), and copper sulfate (1.0 mM, to shorten T1 relaxation time).

The water phantoms were prepared using a binary system of heavy water (D_2O) and deionized water (H_2O), with concentration gradients set at 0 %, 10 %, 20 %, 30 %, 40 %, 50 %, 70 %, 90 %, and 100 % H_2O to simulate the physiological range of water content in biological tissues (the 0 %–100 % range comprehensively covers the physiological water content spectrum of human soft tissues). The use of deionized H_2O is essential to eliminate interference from ionic or organic impurities that could alter proton relaxation times (T_1, T_2) or introduce signal artifacts, thereby ensuring that the observed MRI signal intensity is solely

Fig. 1. (a) Prepared fat phantom and water phantom and (b) Preparation process diagram of the fat solution.

correlated with the concentration of water molecules. Heavy water (D_2O) serves as a "zero-signal" reference, as deuterium (^2H) does not produce detectable signals in ^1H MRI, enabling precise calibration of the signal intensity scale from 0 % (pure D_2O) to 100 % (pure deionized H_2O).

To ensure experimental stability, all test solutions were placed in the scanning room for ≥30 min before imaging to reach thermal equilibrium (25 °C ± 0.5 °C). During data acquisition, nine standard glass vials [20-mm diameter × 50-mm height] were aligned and fixed at the isocenter of the phased-array body coil. Method validation included three independent scans over 72 h (at intervals of 24 and 48 h after the first scan).

2.4. Biological sample preparation and imaging

During the experiment, a standardized sample processing protocol was strictly followed. Five fresh chicken breast samples were purchased and stored in a freezer immediately after purchase. Chicken breast was selected as the biological sample for this study primarily due to three key considerations: first, it is a typical soft tissue with a well-characterized "water–lipid–protein" ternary composition (consistent with the theoretical framework of this study) and low inter-individual variability in elemental content, which minimizes confounding factors in quantitative validation; second, its high homogeneity and relatively simple tissue structure avoid interference from complex components (e.g., connective tissue, glands) that may affect MRI signal quantification, ensuring reliable mapping between molecular contents and elemental mass fractions; third, as an in vitro soft tissue biomimetic material, chicken breast offers advantages such as affordability, easy availability, simple storage, and high batch consistency. Before each scan, the samples were thawed in a refrigerator for 5 h and then allowed to reach thermal equilibrium in the scanning room to ensure measurement consistency. For imaging, a continuous scanning approach was adopted: MRI was performed first, followed immediately by CT scanning to maintain consistent sample conditions between the two measurements. As previously mentioned, the MRI parameters were fixed. CT imaging was performed using a Philips Brilliance CT scanner with the following parameters: tube voltage 120 kVp, tube current-time product 395 mAs, slice thickness 2.5 mm, standard(B) reconstruction kernel, iterative reconstruction (iDose4, level 3), and a pixel matrix of 512 × 512.To obtain accurate reference data, the scanned samples were sent to a professional testing laboratory for elemental analysis using a high-precision element analyzer (EA) (Werner and Brand, 2001) with a measurement accuracy of ≤0.3 %.

2.5. Data processing and statistical analysis

In the fat quantification validation experiment, the built-in fat quantification function of the Philips MRI system was used to delineate the regions of interest (ROIs) and obtain fat mass fraction values. To evaluate the repeatability of the measurements systematically, a Bland–Altman (Bland and Altman, 1986) agreement analysis was performed on datasets from three independent scans. During the establishment of the water content calibration curve, the water-phase images acquired using the mDIXON-Quant sequence exhibited intensity inhomogeneity (bias field artifacts) unrelated to the actual anatomical structure. These artifacts were caused by the inherent hardware limitations of the scanner and unavoidable magnetic field inhomogeneity during imaging. The N4 correction algorithm (Tustison et al., 2010) was applied to suppress these artifacts before the quantitative analysis. Image postprocessing was performed using ImageJ software (Schneider et al., 2012) and included the following steps: (1) grayscale normalization of the corrected images and (2) establishing a calibration relationship between the image grayscale values and water concentration using linear regression analysis.

In bioimaging analysis, when processing the MRI scan results, the water and fat mass fractions of the samples were first measured precisely using fat quantification technology and standardized water content calibration curves. The protein mass fraction was subsequently calculated based on the normalization constraint that the mass fractions of water, lipid, and protein sum to unity. Using known elemental composition ratios of biological molecules, the mass fractions of four elements—C, H, O, and N— were then derived. For the CT scan analysis, the Neumanta treatment planning system(Chen et al., 2022) (a next-generation specialized platform for BNCT developed by Neuboron Medical Group) was employed. The software first reads the patient CT image data and then uses its built-in material conversion algorithm to map HU values to specific human tissue composition information.

3. Results

3.1. Validation of MRI-based fat quantification

As shown in Fig. 2a, the quantitative analysis of fat phantoms based on the mDIXON-Quant sequence demonstrated excellent agreement between the MRI-measured fat mass fraction values and the theoretical expected values across all samples (mean relative deviation <0.1 %). These results validate the quantitative accuracy of the measurement system. Error analysis from three independent reproducibility experiments showed that the standard deviation of the measurements (represented by error bars) remained consistently within a narrow range. This further confirms the measurement repeatability and data reliability of this technical approach.

To evaluate the consistency of the experimental results, a Bland–Altman analysis was performed on three scan datasets. Pairwise comparisons showed that the majority of data points fell within the 95 % limit of agreement and were evenly distributed (Fig. 2b), indicating measurement consistency between different operators and supporting their interchangeability. These findings validate the reliability and repeatability of the mDIXON-Quant technology for fat quantification.

3.2. Establishment and validation of water content calibration curves

Using pre-prepared D_2O/H_2O phantom solutions, a quantitative calibration relationship was established between MRI image grayscale values and known water mass fractions (Fig. 3a). Linear regression analysis demonstrated a strong linear correlation between the grayscale signal intensity and reference water mass fraction ($R^2 > 0.99$, $p < 0.001$), confirming the methodological feasibility of water mass fraction quantification based on MRI grayscale values.

To validate the accuracy of the calibration model systematically, six additional water phantom samples were prepared with varying concentration gradients (range: 34–70 %), each measured twice independently (n = 2). Using the calibration curve ($y = 0.01015x + 4.35281 \times 10^{-4}$) for reverse calculation, all samples showed excellent agreement between measured and theoretical water mass fractions (Fig. 3b). Quantitative analysis revealed an average relative deviation of less than 0.1 %, further confirming the accuracy and reliability of this method.

3.3. Validation of MRI-based elemental quantification using biological samples

To evaluate the accuracy of the proposed MRI method for the quantitative analysis of the elemental composition in biological tissues, five fresh chicken breast samples were analyzed systematically. Based on the theoretical framework of "human soft tissue–molecular content–elemental mass fraction", the mass fraction of four elements (C, H, O, and N) were derived using MRI technology, with EA measurements serving as reference standards. The experimental results (Tables 3 and 4) showed good agreement between MRI-derived and reference values for H, N, and O, with relatively small deviations. However, the measurements of C exhibited some instability. These findings preliminarily demonstrate that the MRI-based framework can achieve non-destructive

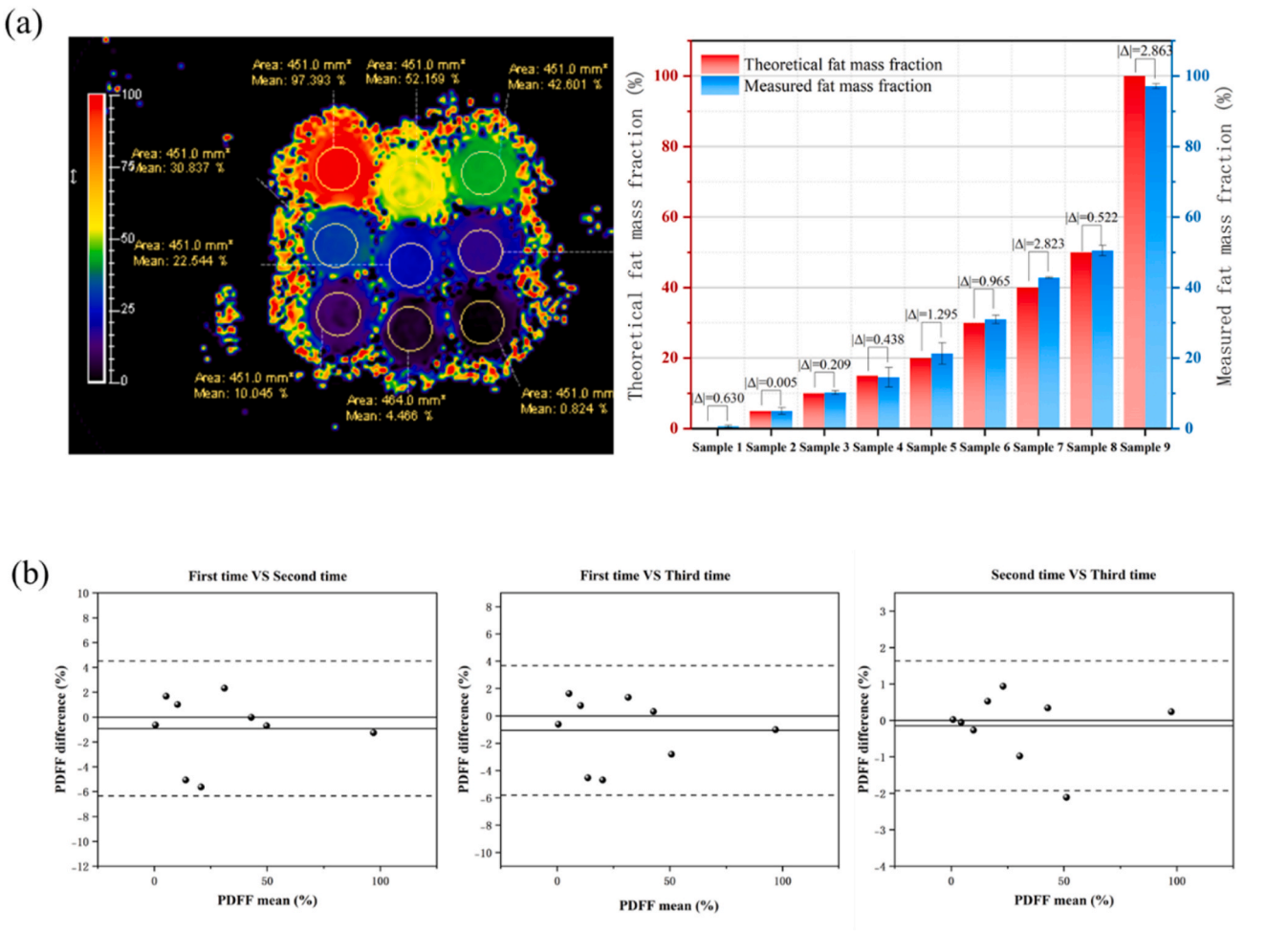

Fig. 2. (a) Fat quantification operation page and the measurement result of fat mass fraction in the lipid solution (The numbers in the figure represent the absolute differences between groups) and (b) consistency test chart for three measurements (Bland–Altman plot).

quantitative detection of the elemental composition in soft tissues.

3.4. Performance comparison of MRI and CT in elemental composition analysis

To evaluate the advantages of the proposed MRI-based method, its performance was compared directly with that of conventional CT for EA. As shown in Fig. 4, the MRI method demonstrated significantly better accuracy in predicting elemental mass fraction than the CT gold standard. MRI revealed markedly reduced absolute deviations for C, H, and N, with a particularly improvement in N quantification. However, no significant difference was observed for O measurements between the two methods. These results indicate that MRI provides a more precise quantification of soft-tissue elemental composition, offering more accurate tissue parameters for MC simulations and reducing systematic errors in dose calculations. In addition, MRI offers the advantage of being radiation-free, making it more suitable for repeated imaging and clinical applications in radiation-sensitive populations. The superior soft-tissue contrast of MRI enhances the precision of organ-at-risk (OAR) delineation, which is crucial for minimizing normal tissue toxicity in BNCT.

4. Discussion

This study is based on a simplified "water-lipid-protein" ternary theoretical model validated using standard human tissue datasets. This theoretical framework enables the quantitative conversion of molecular mass fractions measured via MRI into mass fractions of C, H, O, and N. During the construction of the methodology, a simplified oil-water binary model was primarily employed, which may raise questions regarding its reliability in real tissues. From the perspective of MRI physics, the signals acquired by chemical-shift-based water-fat separation techniques (such as mDIXON-Quant) originate mainly from the mobile proton pool with relatively long transverse relaxation times (T2). Although macromolecules such as glycogen and proteins also contain abundant hydrogen atoms, their protons are restricted within rigid molecular structures, resulting in highly constrained motion and extremely strong dipole–dipole interactions, which lead to very short T_2 relaxation times (typically on the order of microseconds) (Ernst RR, 1992). The echo times (TE) used in clinical MRI sequences (generally in the millisecond range) are far longer than the T2 of these solid-state protons (Boesch C et al., 2002). Consequently, the magnetization from such components decays completely before signal acquisition begins and cannot produce detectable MR signals. Therefore, within the signal model of Dixon-based techniques, the observable signals arise solely from mobile water protons and mobile fat protons, which physically justifies the use of a simplified model for method development.

The validation results of the constructed system indicate that the mDIXON-Quant technique achieves high precision in fat quantification. It should be noted that the PDFF reported by the MRI scanner is not strictly equivalent to the mass fraction of fat; however, in this study, PDFF was employed as a surrogate measure for the fat mass fraction. First, a substantial body of research (Tang A. et al., 2013; Idilman IS. et al., 2013; Kang BK. et al., 2018) has demonstrated good correlation

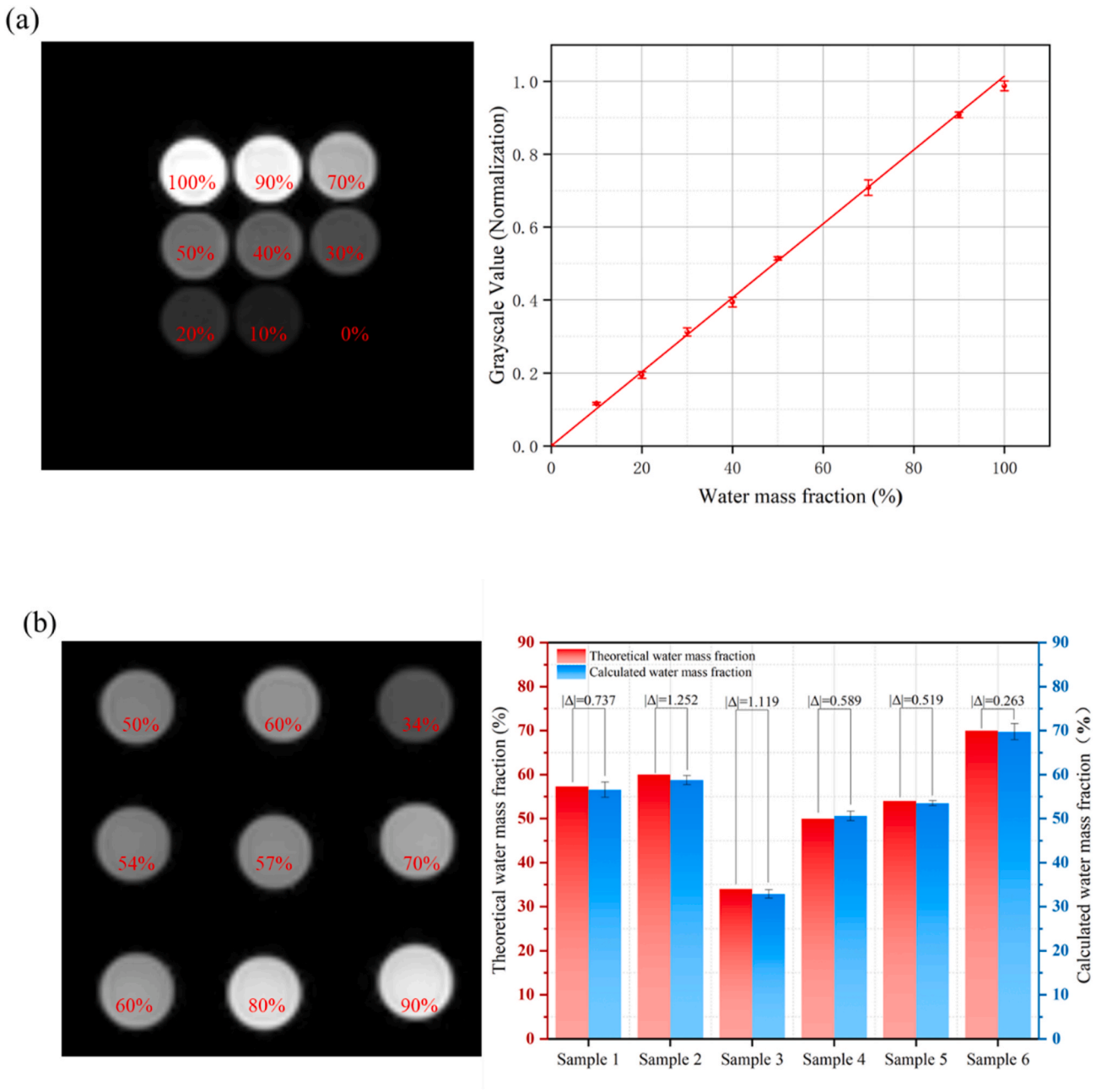

Fig. 3. (a) Water-phantom grayscale image from MRI scan and water content calibration curve and (b) water-phantom grayscale image from MRI scan and validation results of water mass fraction back-calculation (The numbers in the figure represent the absolute differences between groups).

Table 3
Comparison of soft-tissue H and C mass fractions measured by different methods (values in parentheses are absolute differences).

Methods	EA		CT-based method		MRI-based method	
	H(%)	C(%)	H(%)	C(%)	H(%)	C(%)
1	10.030	13.950	10.79	22.324	9.836	22.850
			(0.76)	(8.374)	(0.194)	(8.900)
2	10.830	13.910	11.691	25.125	10.214	16.926
			(0.861)	(11.215)	(0.616)	(3.016)
3	11.570	11.90	10.26 0	21.056	10.632	15.110
			(1.310)	(9.156)	(0.938)	(3.210)
4	9.280	18.080	11.691	25.125	10.214	16.926
			(2.411)	(7.045)	(0.934)	(1.154)
5	11.880	13.030	10.016	21.200	10.820	18.213
			(1.864)	(8.170)	(1.060)	(5.183)

Table 4
Comparison of soft-tissue N and O mass fractions measured by different methods (values in parentheses are absolute differences).

Methods	EA		CT-based method		MRI-based method	
	N(%)	O(%)	N(%)	O(%)	N(%)	O(%)
1	4.400	64.060	2.408	64.307	5.393	61.584
			(1.992)	(0.247)	(0.993)	(2.476)
2	4.310	66.440	2.603	69.501	3.913	68.702
			(1.707)	(3.061)	(0.397)	(2.262)
3	3.800	66.890	2.657	65.437	3.693	70.705
			(1.143)	(1.453)	(0.107)	(3.815)
4	4.360	58.790	2.603	69.501	3.913	68.702
			(1.757)	(10.711)	(0.447)	(9.912)
5	4.140	65.850	2.252	65.590	4.624	66.858
			(1.888)	(0.260)	(0.484)	(1.008)

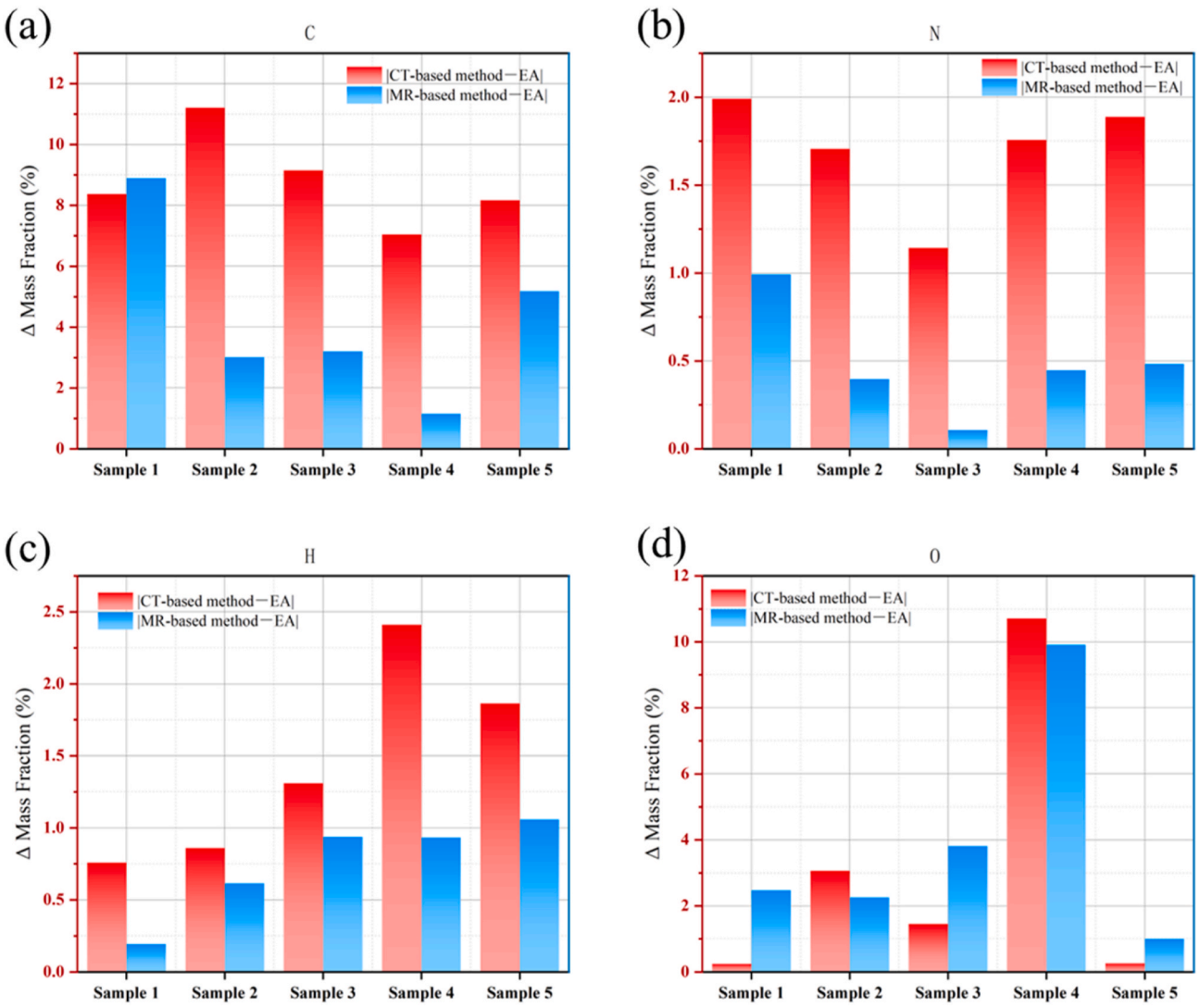

Fig. 4. (a)–(d) Absolute deviations (Δ) in the mass fractions of C, N, H, and O between the MRI/CT methods and the reference standard of elemental analysis (EA).

and consistency between PDFF obtained via Dixon-based quantitative techniques and histological or phantom-based reference fat contents, such as biopsy or magnetic resonance spectroscopy (MRS) results. Second, the experimental results in Section 3.1 show that the measured fat mass fraction (actually PDFF) is highly consistent with the theoretical fat mass fraction, thereby further supporting the reliability of this substitution. Furthermore, we evaluated the impact of directly using PDFF as the fat mass fraction (neglecting differences in hydrogen density) on the final elemental composition calculation using a conservative binary model. The analysis showed that even under an extreme scenario with a relative error of ±10 % in PDFF, the resulting deviations in the calculated mass fractions of C, H, O, and N were all less than 0.5 %. In a realistic ternary system (water-lipid-protein), the hydrogen contribution from proteins would further reduce the discrepancy between PDFF and the true fat mass fraction. Hence, the binary-model-based assessment is conservative, and the actual error is likely smaller. Overall, the direct use of PDFF as the fat mass fraction in this study is both reasonable and effective.

Nevertheless, some measurement errors remain in the experiments, primarily stemming from solution non uniformity caused by unavoidable human related variations during solution preparation. The calibration model for water mass fraction exhibited excellent linearity ($R^2 > 0.99$), although a slight systematic underestimation was observed at 100 % water content, likely attributable to signal intensity saturation effects at high water concentrations. Given that only a limited proportion of organs in human tissues possess such high water content, the impact of this systematic error on overall measurements remains within an acceptable range.

The experimental data show that the MRI-measured mass fractions of H, N, and O agree well with the EA results, with relatively small deviations. However, the quantification of C showed significant instability with larger deviations. This variability may be caused by complex molecular structures and the difficulty in mapping MRI signals to C mass fraction. To evaluate how elemental quantification errors affect BNCT dose calculations, a dose sensitivity analysis was performed using clinical cases of patients with head and neck cancer. During dose planning, the mass fractions of C, H, O, and N were adjusted independently to measure their individual effects on the final dose. The results indicated that even a 30% change in C mass fraction had the smallest effect on dose calculation (<1.5 %), whereas variations in H, N, and O had more-significant influences on dose distribution. Therefore, although MRI-based C quantification has certain limitations, its impact on the overall accuracy of BNCT dose calculation is negligible.

Compared with CT-based methods, MRI offers several advantages for soft tissue EA. The improved accuracy in predicting the mass fractions of C, H, and N demonstrates that MRI can provide more reliable tissue parameters for MC simulations, thereby reducing systematic errors in dose calculations. In addition, the radiation-free nature of MRI makes it

suitable for repeated imaging and applications in radiation-sensitive populations. Its superior soft tissue contrast also makes better delineation of OARs possible, which is crucial for minimizing normal tissue toxicity in BNCT.

The main limitations and future research directions center on four key aspects: (1) To further validate the feasibility of the oil–water binary model, future research will develop multi-component models that incorporate biomacromolecules such as proteins, in order to more accurately simulate tissue complexity. It is also planned to validate the proposed method using a wider range of ex vivo and in vivo biological tissue samples, thereby systematically assessing its robustness under realistic biological conditions. (2) The current method cannot provide voxel-level elemental distribution maps or fully quantify elements in bone. Future work should explore integrating CT with MRI images to develop a more comprehensive imaging system. (3) Measurements of C exhibited substantial variability. Optimization of MRI sequences or the incorporation of complementary methods (such as spectroscopy) is needed to improve the quantification of C element. (4) Direct integration of MRI-derived tissue parameters into BNCT treatment planning remains a prospective research direction. The feasibility and accuracy of such integration must be validated through patient-specific imaging combined with dose calculation. Future research should focus on addressing these issues to refine the MRI-based system, thereby supporting more precise BNCT treatment planning.

5. Conclusions

The feasibility and advantages of using MRI-based quantitative analysis for determining soft tissue elemental composition in BNCT dose calculations were demonstrated. By applying mDIXON-Quant MRI technology, a reliable framework was developed to quantify water, lipid, and protein mass fraction, from which the mass fractions of important elements (C, H, O, and N) were derived. The results showed that MRI outperformed conventional CT methods in determining the mass fractions of critical elements such as H and N, both of which are essential for BNCT dose calculations. Although promising, this study is only a preliminary step. The observed variability in C quantification highlights an area that requires improvement in future studies. Further research is needed to extend this method to other tissue types. Subsequent efforts should focus on integrating multimodal imaging and advanced spectroscopy techniques to achieve voxel-level elemental mapping and broader clinical validation.

CRediT authorship contribution statement

Guolong Liu: Writing – original draft, Data curation, Conceptualization. **Diyun Shu:** Writing – review & editing, Supervision, Methodology, Funding acquisition, Formal analysis, Conceptualization. **Changran Geng:** Writing – review & editing, Supervision, Methodology. **Xiaobin Tang:** Writing – review & editing. **Yuan-Hao Liu:** Writing – review & editing. **Yingzhi Zheng:** Investigation. **Junhang Gao:** Investigation. **Sulian Su:** Resources. **Youqun Lai:** Resources.

Declaration of competing interest

The authors declare that they have no known competing financial interests or personal relationships that could have appeared to influence the work reported in this paper.

Acknowledgements

This work was supported by National Natural Science Foundation of China (grant No. 12261131621, 12220101005). We acknowledge the Imaging Center of Xiamen Humanity Hospital for providing equipment support.

Data availability

Data will be made available on request.

References

Andreo, P., 1991. Monte carlo techniques in medical radiation physics. Phys. Med. Biol. 36, 861–920. http://iopscience.iop.org/0031-9155/36/7/001.

Andreo, P., 2018. Monte carlo simulations in radiotherapy dosimetry. Radiat. Oncol. 13, 121. https://doi.org/10.1186/s13014-018-1065-3.

Bland, J.M., Altman, D.G., 1986. Statistical methods for assessing agreement between two methods of clinical measurement. Int. J. Nurs. Stud. 47, 931–936. https://doi.org/10.1016/j.ijnurstu.2009.10.001.

Barth, R.F., Soloway, A.H., Fairchild, R.G., et al., 1992. Boron neutron capture therapy for cancer. Realities and prospects. Cancer 70, 2995–3007. https://www.jstor.org/stable/24997067.

Boesch, C., Kreis, R., 2002. Dipolar coupling and ordering effects observed in magnetic resonance spectra of skeletal muscle. NMR Biomed. 15 (7–8), 488–500. https://doi.org/10.1002/nbm.684.

Barth, R.F., H, Vicente Mg, Harling, O.K., et al., 2012. Current status of boron neutron capture therapy of high grade gliomas and recurrent head and neck cancer. Radiat. Oncol. 7, 146. https://doi.org/10.1186/1748-717X-7-146.

Barth, R.F., Mi, P., Yang, W., 2018. Boron delivery agents for neutron capture therapy of cancer. Cancer Commun. 38, 1–15. https://doi.org/10.1186/s40880-018-0299-7.

Chen, J., Teng, Y.C., Zhong, W.B., et al., 2022. Development of Monte Carlo based treatment planning system for BNCT. J. Phys., Conf. Ser. 2313, 012012. https://doi.org/10.1088/1742-6596/2313/1/012012.

Ernst, R.R., 1992. Nuclear magnetic resonance fourier transform spectroscopy (nobel lecture). Angew. Chem. Int. Ed. 31 (9), 1010–1024. https://doi.org/10.1002/anie.199208053.

Grevillot, L., Frisson, T., Zahra, N., et al., 2010. Optimization of GEANT4 settings for proton pencil beam scanning simulations using GATE. Nucl. Instrum. Methods Phys. Res. Sect. B Beam Interact. Mater. Atoms 268, 3295–3305. https://doi.org/10.1016/j.nimb.2010.07.011.

Giera, M., 2020. In: Griffiths, W., Wang, Y. (Eds.), Lipidomics: Current and Emerging Techniques, first ed. Springer, Cham, pp. 7371–7372. https://doi.org/10.1007/s00216-020-02871-7.

Hernando, D., Hines, C.D.G., Yu, H., et al., 2012. Addressing phase errors in fat-water imaging using a mixed magnitude/complex fitting method. Magn. Reson. Med. 67, 638–644. https://doi.org/10.1002/mrm.23044.

Hünemohr, N., Paganetti, H., Greilich, S., et al., 2014. Tissue decomposition from dual energy CT data for MC based dose calculation in particle therapy. Med. Phys. 41, 061714. https://doi.org/10.1118/1.4875976.

Hernando, D., Wells, S.A., Vigen, K.K., et al., 2015. Effect of hepatocyte-specific gadolinium-based contrast agents on hepatic fat-fraction and R2. Magn. Reson. Imaging 33, 43–50. https://doi.org/10.1016/j.mri.2014.10.001.

Hernando, D., Sharma, S.D., Aliyari, Ghasabeh M., et al., 2017. Multisite, multivendor validation of the accuracy and reproducibility of proton-density fat-fraction quantification at 1.5T and 3T using a fat-water phantom: proton-density fat-fraction quantification at 1.5T and 3T. Magn. Reson. Med. 77, 1516–1524. https://doi.org/10.1002/mrm.26228.

Idilman, I.S., Aniktar, H., Idilman, R., et al., 2013. Hepatic steatosis: quantification by proton density fat fraction with MR imaging versus liver biopsy. Radiology 267 (3), 767–775. https://doi.org/10.1148/radiol.13121360.

Kumada, H., Takada, K., 2018. Treatment planning system and patient positioning for boron neutron capture therapy. Ther. Radiol. Oncol. 2. https://doi.org/10.21037/tro.2018.10.12, 50-50.

Kang, B.K., Kim, M., Song, S.Y., 2018. Feasibility of modified Dixon MRI techniques for hepatic fat quantification in hepatic disorders: validation with MRS and histology. Br. J. Radiol. 91 (1089), 20170378. https://doi.org/10.1259/bjr.20170378.

Lins, C.F., Salmon, C.E.G., Nogueira-Barbosa, M.H., 2021. Applications of the Dixon technique in the evaluation of the musculoskeletal system. Radiol. Bras. 54, 33–42. https://doi.org/10.1590/0100-3984.2019.0086.

Smith, M.H., 1966. The amino acid composition of proteins. J. Theor. Biol. 13, 261–282. https://doi.org/10.1016/0022-5193(66)90021-X.

Schneider, U., Pedroni, E., Lomax, A., 1996. The calibration of CT hounsfield units for radiotherapy treatment planning. Phys. Med. Biol. 41, 111–124. http://iopscience.iop.org/0031-9155/41/1/009.

Schneider, W., Bortfeld, T., Schlegel, W., 2000. Correlation between CT numbers and tissue parameters needed for monte carlo simulations of clinical dose distributions. Phys. Med. Biol. 45, 459–478. http://iopscience.iop.org/0031-9155/45/2/314.

Sauerwein, W., Wittig, A., Moss, R., et al., 2012. Neutron Capture Therapy - Principles and Applications. Springer. https://doi.org/10.1007/978-3-642-31334-9_1.

Sudhyadhom, A., 2020. On the molecular relationship between hounsfield unit (HU), mass density, and electron density in computed tomography (CT). PLoS One 15, e0244861. https://doi.org/10.1371/journal.pone.0244861.

Saito, M., Matsumoto, R., 2023. Technical note: implementing MRI/CT-based elemental concentration data to monte carlo simulation for yielding positron emitters in proton therapy. Med. Phys. 41, 071701. https://doi.org/10.1118/1.4881327.

Saito, M., 2023. MRI-based quantification of carbon and oxygen concentrations in human soft tissues for range verification in proton therapy. Med. Phys. 50, 5671–5681. https://doi.org/10.1002/mp.16353.

Schneider, C.A., Rasband, W.S., Eliceiri, K.W., 2012. NIH image to ImageJ: 25 years of image analysis. Nat. Methods 9, 671–675. https://doi.org/10.1038/nmeth.2089.

Tustison, N.J., Avants, B.B., Cook, P.A., et al., 2010. N4ITK: improved N3 bias correction. IEEE Trans. Med. Imag. (29), 1310–1320. https://doi.org/10.1109/TMI.2010.2046908.

Tang, A., Tan, J., Sun, M., et al., 2013. Nonalcoholic fatty liver disease: MR imaging of liver proton density fat fraction to assess hepatic steatosis. Radiology 267 (2), 422–431. https://doi.org/10.1148/radiol.12120896.

Teng, Y.C., Chen, J., Zhong, W.B., et al., 2023. HU-based material conversion for BNCT accurate dose estimation. Sci. Rep. 13, 15701. https://doi.org/10.1038/s41598-023-42508-0.

Woodard, H.Q., White, D.R., 1986. The composition of body tissues. Br. J. Radiol. 59, 1209–1218. https://doi.org/10.1259/0007-1285-59-708-1209.

Werner, R.A., Brand, W.A., 2001. Referencing strategies and techniques in stable isotope ratio analysis. Rapid Commun. Mass Spectrom. 15, 501–519. https://doi.org/10.1002/rcm.258.

Zhong, W.B., Cheng, J., Teng, Y.C., et al., 2023. Introduction to the monte carlo dose engine COMPASS for BNCT. Sci. Rep. 13, 11965. https://doi.org/10.1038/s41598-023-38648-y.